

# Rhodium Dispersion in a Rh/Ce<sub>0.68</sub>Zr<sub>0.32</sub>O<sub>2</sub> Catalyst Investigated by HRTEM and H<sub>2</sub> Chemisorption

Jose M. Gatica,<sup>†</sup> Richard T. Baker,<sup>‡,§</sup> Paolo Fornasiero,<sup>†</sup> Serafin Bernal,<sup>‡</sup> Ginesa Blanco,<sup>‡</sup> and Jan Kašpar<sup>\*,†</sup>

*Dipartimento di Scienze Chimiche, Università di Trieste, Via Giorgieri 1, Trieste 34127, Italy, and Departamento de Ciencia de los Materiales e Ingeniería Metalúrgica y Química Inorgánica, Facultad de Ciencias, Universidad de Cádiz, Avda. de la Republica Saharaui s/n, Apdo. 40. E-11510, Puerto Real (Cádiz), Spain*

*Received: November 17, 1999; In Final Form: February 18, 2000*

The effect of reduction temperature on the hydrogen adsorption and Rh dispersion in a Rh/Ce<sub>0.68</sub>Zr<sub>0.32</sub>O<sub>2</sub> catalyst with texturally stable Ce<sub>0.68</sub>Zr<sub>0.32</sub>O<sub>2</sub> support was investigated. Rh dispersion data were also obtained from Rh particle size analyses made using high-resolution transmission electron microscopy (HRTEM) images. Comparison of the dispersion values obtained by using the two techniques showed that H<sub>2</sub> adsorption at -80 °C is a suitable tool for the estimation of Rh dispersion at reduction temperature,  $T_{\text{red}}$ ,  $\leq 500$  °C. For  $T_{\text{red}} > 500$  °C, a partial suppression of H<sub>2</sub> chemisorption was observed. However, after a mild reoxidation and low temperature reduction, the H<sub>2</sub> adsorption capacity of these samples was regenerated and good agreement with the HRTEM data was again obtained.

## 1. Introduction

H<sub>2</sub> chemisorption has long been used as a valuable technique for the rapid measurement of the exposed metal surface area, and hence the estimation of mean particle size, of supported metal particles.<sup>1</sup> This method has undergone severe criticism, because the underlying assumptions regarding the H/NM (NM = noble metal) stoichiometry and the particle geometry may not be valid, especially for very small particles. Nevertheless, because of its simplicity and cheapness, it is certainly the most widely used method. NM/CeO<sub>2</sub>-Al<sub>2</sub>O<sub>3</sub> systems have been used widely as catalysts for automotive pollution control, which makes them materials of strong interest.<sup>2</sup> Nowadays, the so-called three-way catalyst (TWC) containing NM (Rh, Pd, and Pt), CeO<sub>2</sub>-ZrO<sub>2</sub> mixed oxides, and Al<sub>2</sub>O<sub>3</sub> as main constituents is used to remove NO<sub>x</sub>, CO, and hydrocarbons from the exhaust gases.<sup>2,3</sup> The importance of Rh in promoting NO<sub>x</sub> removal and the ability of the NM in conjunction with CeO<sub>2</sub>, and later on with CeO<sub>2</sub>-ZrO<sub>2</sub> mixed oxides, to promote the oxygen storage/release capacity have long been recognized as important factors in determining the efficiency of the TWCs.<sup>4-6</sup> The latter property, which is achieved by the facile Ce<sup>4+</sup>/Ce<sup>3+</sup> interconversion, is a crucial one for the TWCs because it allows one to keep the air-to-fuel ratio near stoichiometric conditions, where the highest conversions are attained.<sup>4</sup> The effects of metal dispersion on the interactions between the NM and the CeO<sub>2</sub>, which favorably affect the pollutant conversions, have been clearly established.<sup>7</sup> This makes of interest the determination of the dispersion and morphology of the active NM particles in the NM/CeO<sub>2</sub>-ZrO<sub>2</sub> systems. In the case of CeO<sub>2</sub>-containing catalysts, there is a difficulty in measuring the active metal area

because of significant adsorption of H<sub>2</sub> on the CeO<sub>2</sub> itself.<sup>8-11</sup> In fact, the hydrogen spillover phenomena experienced by the CeO<sub>2</sub>-based catalysts lead to experimental H/NM values that are much higher than those commensurate with the true hydrogen adsorption on the metal.<sup>9</sup> In an early paper, Bernal et al. showed that the measurement of H<sub>2</sub> chemisorption at -80 °C allows measurement of the true H/Rh ratio because no significant spillover occurs at such low temperatures.<sup>10</sup> On the other hand, Fornasiero et al. have shown that prolonged thermal evacuation treatment allows determination of H<sub>2</sub> chemisorption on metal particles dispersed over ceria-zirconia solid solutions.<sup>12,13</sup> However, Cl-containing metal precursors were used in these studies. It is well known that Cl is a strong hydrogen spillover killer, being strongly retained on CeO<sub>2</sub>, thus affecting the H<sub>2</sub> chemisorption properties of the oxide support.<sup>10,14</sup> Measurement of true H/Rh values in these systems is particularly difficult when Rh(NO<sub>3</sub>)<sub>3</sub> is used as a precursor because it has been shown that hydrogen spillover in the final catalyst is much more significant than in catalysts prepared using the RhCl<sub>3</sub> precursor.<sup>15</sup> CO has also been used as a probe molecule; however, adsorption on ceria itself or promoted by a spillover process was found in NM/CeO<sub>2</sub> catalysts.<sup>16,17</sup> Very recently, a pulse CO chemisorption at -78 °C was observed not to be a reliable method.<sup>18</sup> In view of such difficulties, alternative methodologies such as benzene hydrogenation have been suggested as a tool for determining exposed metal surface area in NM/CeO<sub>2</sub> systems.<sup>19</sup>

In this paper, a H<sub>2</sub> chemisorption method combining low temperature and low H<sub>2</sub> pressures is used to measure the Rh metal dispersion in a Rh/Ce<sub>0.68</sub>Zr<sub>0.32</sub>O<sub>2</sub> catalyst. Rh dispersion data obtained by performing a Rh particle size distribution analysis<sup>20</sup> on high-resolution transmission electron microscopy (HRTEM) images of the catalyst samples were used to evaluate the reliability of this methodology. In addition, a study of the effect of temperature of reduction of the catalyst on H<sub>2</sub> adsorption and Rh dispersion has been performed to obtain

\* Corresponding author. Fax: +39-040-6763903; e-mail: Kaspar@univ.trieste.it.

<sup>†</sup> Università di Trieste

<sup>‡</sup> Universidad de Cádiz.

<sup>§</sup> Now at Department of Chemistry, University of Dundee, Nethergate, Dundee DD1 4HN, U.K.

insights into the nature of the metal–support interaction. This point is still matter of debate in the CeO<sub>2</sub>-based systems.<sup>16,21</sup> It is worth noting that, under real exhaust conditions, the modern TWCs experience rich-to-lean (i.e. reducing-to-oxidizing) excursions over an extended range of temperatures, up to 1000 °C.<sup>3</sup>

## 2. Experimental Section

Rh(0.78 wt %)/Ce<sub>0.68</sub>Zr<sub>0.32</sub>O<sub>2</sub> (hereinafter denoted Rh/CZ) was obtained from Rhodia Recherches in the framework of the CEZIRENCAT Project. The CEZIRENCAT project is a multilaboratory project in the area of three-way catalysis funded by the European Union. (Home page <http://www.dsch.univ.trieste.it/cezirencat/index.html>.) Ce<sub>0.68</sub>Zr<sub>0.32</sub>O<sub>2</sub> was characterized in a previous study.<sup>22</sup> It is a CeO<sub>2</sub>-ZrO<sub>2</sub> solid solution with a Brunauer–Emmett–Teller (BET) surface area of 23 m<sup>2</sup> g<sup>-1</sup>, cumulative pore volume 0.167 cm<sup>3</sup> g<sup>-1</sup>, and no microporosity. The mixed oxide was impregnated with a Rh(NO<sub>3</sub>)<sub>3</sub>·*n*H<sub>2</sub>O metal precursor by the incipient wetness impregnation technique. The catalyst was dried at 110 °C and then calcined in a flow of dry air at 450 °C for 5 h.

An in situ cleaning procedure was applied before performing the experiments.<sup>23</sup> The samples were heated in O<sub>2</sub>(5%)/Ar (60 mL min<sup>-1</sup>) from room temperature to 550 °C at a heating rate of 10 °C min<sup>-1</sup>, held at 550 °C for 1 h, and then allowed to cool slowly to room temperature.

The temperature-programmed reduction (TPR) in a H<sub>2</sub>(5%)/Ar (25 mL min<sup>-1</sup>) mixture was performed as previously described.<sup>15</sup> A quadrupole mass spectrometer (VG Sensorlab with PostSoft analysis software), 0.2 g of sample, and a heating rate of 10 °C min<sup>-1</sup> were used.

H<sub>2</sub> chemisorption and BET surface area measurements were conducted using a Micromeritics ASAP 2000 automatic analyzer. H<sub>2</sub> chemisorption experiments were performed at -80 and 25 °C using 0.5 g of sample. The apparent equilibrium was considered to be reached when the pressure change was less than 0.01% for 11 consecutive readings taken at 30-s intervals. A range of H<sub>2</sub> pressure of 2–20 Torr was used. Typically 10 points at 2 Torr steps were acquired. Adsorbed volumes were determined by extrapolation of the linear part of the adsorption isotherm to zero pressure. A chemisorption stoichiometry ratio, H:Rh, of 1:1 was assumed.

The H<sub>2</sub> chemisorption study was performed on the same sample, increasing progressively the reduction temperature ( $T_{\text{red}}$ ). After the cleaning procedure, the sample was reduced in a flow of H<sub>2</sub>(5%)/Ar (60 mL min<sup>-1</sup>) by heating the sample from room temperature up to the selected reduction temperature ( $T_{\text{red}}$  = 150, 350, 500, 700 or 900 °C), holding at  $T_{\text{red}}$  for 1 h, and allowing it to cool to room temperature also in flowing H<sub>2</sub>(5%)/Ar. Before conducting the H<sub>2</sub> chemisorption, the sample was evacuated for 4 h at 400 °C, and after each H<sub>2</sub> chemisorption experiment, the sample was reoxidized by heating it from room temperature to 427 °C in a flow of O<sub>2</sub>(5%)/Ar (60 mL min<sup>-1</sup>). In situ BET surface area measurements were carried out using the same equipment.

The transmission electron microscope used was a JEOL 2000 EX instrument equipped with top-entry sample holder and ion-pumping system and operating at 200 kV. The structural resolution of the microscope was 0.21 nm. HRTEM micrographs of initial magnification up to ×600K were obtained using a film camera attached to the instrument. The resulting negatives were developed chemically and selected areas of the negatives were then digitized using a video camera interfaced to a computer running the SEMPER 6+ suite of image analysis software.

Digital diffractogram patterns, or DDPs, were obtained from these digitized images using the same software package.

Five 250–350-mg samples of the Rh/CZ catalyst were reduced by heating them at a rate of 10 °C min<sup>-1</sup> to a reduction temperature of 150, 350, 500, 700 or 900 °C, and maintaining this temperature for a period of 1 h. After this reduction step, the samples were purged in pure He for 1 h at 500 °C or at the reduction temperature if this was above 500 °C. The samples were allowed to cool to room temperature and then cooled further to about -80 °C using an acetone ice cold-trap. At this point, the gas was switched to O<sub>2</sub> (5%)/He and the temperature of the sample was allowed to rise slowly to room temperature. In this way, the sample was passivated and therefore did not undergo uncontrolled reoxidation on its exposure to air when the reactor was opened. The use of this passivation step maintains the metal particles in their reduced metallic state while allowing the controlled reoxidation of the oxide support. For study in the microscope, the samples were deposited from a hexane suspension prepared in an ultrasound bath onto Cu grids of holey carbon film by passing the grids repeatedly through the suspension using tweezers.

By measuring the size (defined as the longest visible width) of a large number of Rh particles from the HRTEM images, particle size distributions and mean particle size data were obtained. The effects of increasing reduction temperature on these factors could therefore be studied. Further, this particle size data were used to estimate values for the dispersion of the metal phase. Dispersion is defined as the ratio of the number of Rh atoms exposed at a particle surface ( $Rh_s$ ) to the total number of Rh atoms present ( $Rh_T$ ). Cumulative dispersion curves are plotted using the particle size data by assuming a certain metal particle geometry (truncated cubooctahedron) and a certain orientation with respect to the oxide support [with {111}-type planes in contact at the interface, assuming face-centered cubic (fcc) crystal structure for both the oxide and the metal].<sup>20</sup> The curves accumulate the contribution of metal particles to the dispersion with increasing particle size and so show the relative importance to the dispersion of different size ranges. The final value, therefore, gives the accumulated dispersion of all the particles measured, which is the estimated value of the overall dispersion for a particular sample.

## 3. Results and Discussion

### 3.1. HRTEM Study. 3.1.1. Rh Particle Size and Dispersion.

Rh particle size distributions and cumulative dispersion curves derived as described above are presented for the samples after reduction at 150, 350, 500, 700 and 900 °C in Figure 1. The mass-corrected mean particle size (based on the mass-fraction in each size range) and the number of particles measured in each sample are also included. The Rh particles in these samples are relatively plentiful, so large numbers could be measured and a good statistical distribution obtained. It can be seen from Figure 1 that the particles are initially small (mass-corrected mean, 2.4 nm in the sample reduced at 150 °C), as would be expected in such materials. As the temperature of reduction is increased, mean particle size increases and the particle size distribution broadens: slightly at  $T_{\text{red}}$  = 500 °C and then more significantly to  $T_{\text{red}}$  = 700 and 900 °C. The dispersion values obtained from the cumulative dispersion curves presented in Figure 1 are summarized in Table 1. This parameter decreases moderately with increasing reduction temperature. In summary, the samples appear to undergo a classic evolution that can be explained by the progressive sintering of the Rh particles.

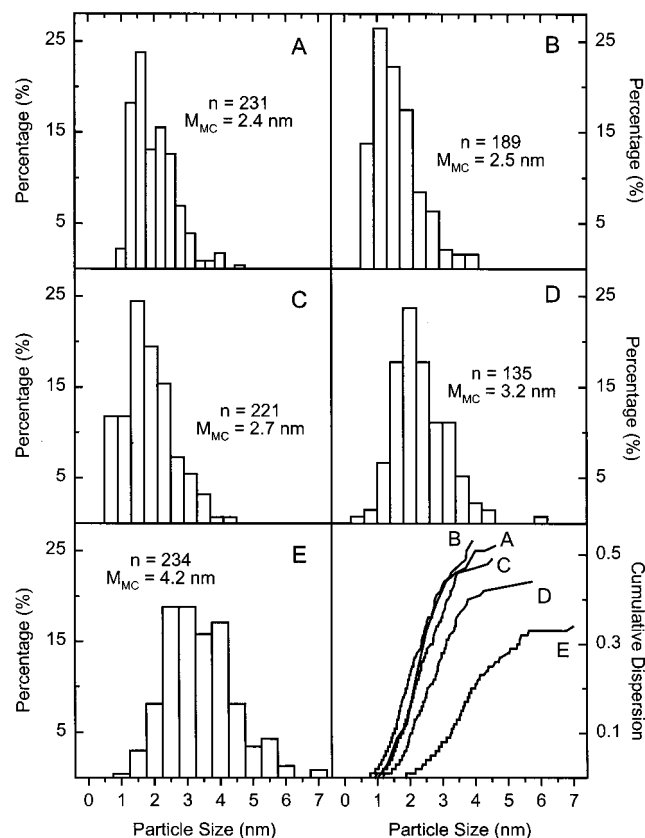


**Figure 1.** Rh particle size distribution histograms for Rh/Ce<sub>0.68</sub>Zr<sub>0.32</sub>O<sub>2</sub> samples reduced at 150 (A), 350 (B), 500 (C), 700 (D), and 900 °C (E), cooled and passivated (as described in text). Number of measured particles (*n*), mass-corrected means (*M*<sub>MC</sub>), and cumulative dispersion plots (right bottom diagram) are also included.

**TABLE 1: Dispersion Data by Means of Volumetric H<sub>2</sub> Chemisorption and HRTEM Studies on Rh/Ce<sub>0.68</sub>Zr<sub>0.32</sub>O<sub>2</sub>**

run <sup>a</sup>	reduction temp. (°C)	H/Rh <sub>T</sub>		Rh <sub>s</sub> /Rh <sub>T</sub> by HRTEM
		25 °C	-80 °C	
1	150	2.38	0.52	0.52
2	350	0.68	0.57	0.53
3	500	0.47	0.49	0.49
4	700	0.38	0.41	0.44
5	150 <sup>b</sup>		0.47	
6	900	0.20	0.23	0.34
7	150 <sup>b</sup>		0.31	

<sup>a</sup> Catalyst evacuated at 400 °C for 4 h before chemisorption measurement. <sup>b</sup> Catalyst from previous experiment, reoxidized at 427 °C and reduced at 150 °C.

**3.1.2. Rh Particle Morphology.** HRTEM images of metal particles in the above samples were examined. Metallic Rh has a fcc structure with a unit cell length of 0.38 nm. This gives rise to interplanar spacing, *d*, of 0.19 and 0.22 nm for the planes of the type {200} and {111}, respectively. Under normal working conditions, the {111} spacing is the only Rh spacing that can be routinely detected by the microscope used, although detection of the {200} spacing is also possible under favorable operating and experimental conditions. Previous work<sup>24</sup> has shown that the Ce<sub>0.68</sub>Zr<sub>0.32</sub>O<sub>2</sub> bare oxide support contains a significant amount of tetragonal phase. However, to allow simple comparisons between the fcc metal structure and that of the oxide the oxide crystallography is also expressed here in terms of fcc symmetry.

In the samples reduced at 150 and 350 °C, the Rh particles are very small and therefore rather difficult to image. However, the taking of DDPs from the relevant sections of the images

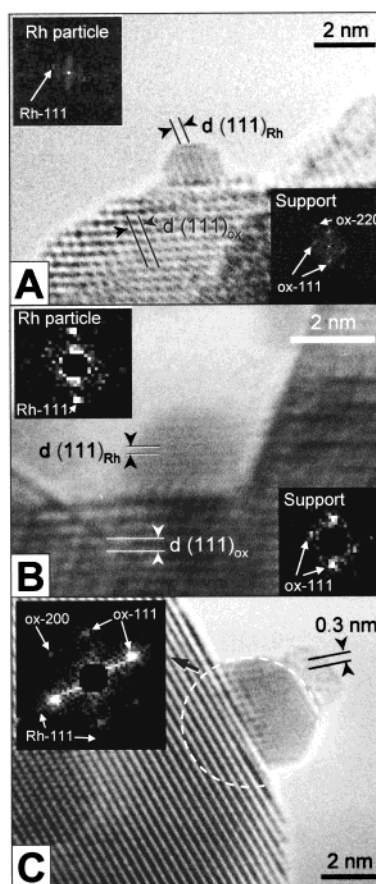


**Figure 2.** HRTEM images of Rh/Ce<sub>0.68</sub>Zr<sub>0.32</sub>O<sub>2</sub> catalyst reduced at 150 (A), 500 (B), and 900 °C (C). DDPs of selected areas with characteristic interplanar spacings of metal and support indicated.

allows the identification of certain Rh and oxide support interplanar spacings. In Figure 2A, {111}-type planes are identified in the bulk of the Rh metal particle and of the Ce<sub>0.68</sub>Zr<sub>0.32</sub>O<sub>2</sub> oxide support for the catalyst reduced at 150 °C. These are labeled Rh-111 and ox-111 respectively, in the DDPs. By reference to the image and the DDP patterns (inset), a structural relationship is seen to exist between the oxide support and the Rh particles consisting of a parallel alignment of planes. This epitaxial relation is also present in the sample after reduction at 500 °C: Figure 2B shows an image of a Rh particle on an oxide support crystal viewed along close to a {011}-type zone axis for the sample reduced at 500 °C. One of the {111}<sub>Rh</sub> planes is seen to be aligned with a {111}<sub>ox</sub> plane. The profile views of the Rh particles obtained for the Rh/CZ catalyst reduced at temperatures up to 500 °C show that they exhibit the regular truncated cubooctahedral morphology that has been found to be typical for Rh-CeO<sub>2</sub> catalysts after treatment in the same range of reduction temperatures.<sup>25</sup> As deduced from the statistical data included in Figure 1(A) through (E), about 200 Rh particles were analyzed in most of cases. Conclusions about particle morphology, metal/support structural relations, and particle size distribution are thus based on a number of observations that allow them to be considered as statistically meaningful. Except where otherwise explicitly stated, micrographs in Figure 2 are also representative of the ensemble of imaged Rh particles. After reduction at 700 and 900 °C, the Rh metal particles are relatively large and easy to image. They maintain the epitaxial relation with the support and their regular morphology. Nevertheless, a new phenomenon is seen in these samples: a small fraction of the metal particles appears to be decorated. A good example of this effect is shown in Figure

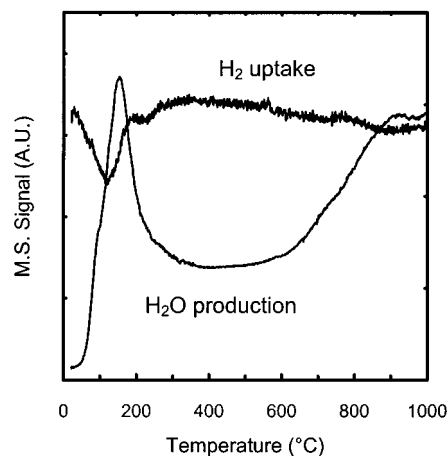


**Figure 3.** H<sub>2</sub> uptake and H<sub>2</sub>O evolution in the TPR of Rh/Ce<sub>0.68</sub>Zr<sub>0.32</sub>O<sub>2</sub> using MS as detector.

2C for the sample reduced at 900 °C. The Rh and support crystals are viewed along tilted  $\langle 110 \rangle$ -type zone axes. The two Rh  $\{111\}$ -type planes are seen to be in alignment with those of the support (see DDP inset). The material decorating the top of the Rh particle appears to consist of planes with  $d = 0.3$  nm, suggesting that this material is an oxide derived from the support and that it possesses similar crystallography, these planes being assigned as  $\{111\}_{\text{ox}}$  type. In this case, these planes appear to be aligned with  $\{111\}_{\text{Rh}}$ -type planes of the Rh particle. Importantly, decoration of the metal phase accounts for less than 5% of the profile-view images of particles detected in the sample reduced at 900 °C. This suggests that decoration would play only a minor role in determining the chemical properties of the catalyst reduced at high temperature.

**3.2. Temperature-Programmed Reduction by Mass Spectrometry Study.** The TPR by mass spectrometry (MS) experiments were aimed at studying the reduction process of the Rh/CZ sample, since it is known that H<sub>2</sub> adsorption is affected by the degree of reduction of the CeO<sub>2</sub>-ZrO<sub>2</sub> support.<sup>13</sup> The TPR-MS profiles for the H<sub>2</sub> uptake and H<sub>2</sub>O evolution of the sample after the cleaning procedure are presented in Figure 3. The plot of H<sub>2</sub> uptake features an intense and broad peak with maximum at 130 °C and a shoulder around 230 °C. There is also a very broad and poorly resolved H<sub>2</sub> uptake feature at high temperatures. All these features can be related to the reduction processes of Rh oxide and the support.<sup>12</sup> The low-temperature peak is attributed to reduction of the dispersed metal phase, probably in the form of Rh<sub>2</sub>O<sub>3</sub> after the treatment with O<sub>2</sub>(5%)/Ar at 550 °C,<sup>26</sup> and a partial reduction of the Ce<sub>0.68</sub>Zr<sub>0.32</sub>O<sub>2</sub> support. The high-temperature features may be associated with the processes of surface/bulk reduction and bulk reduction of the ceria-zirconia solid solution with concomitant vacancy creation and water desorption, in agreement with the trace for water evolution presented in the same Figure 3. The delay in H<sub>2</sub>O production with respect to the H<sub>2</sub> uptake might suggest that H<sub>2</sub> adsorption precedes the reduction/oxygen vacancy creation step. However, delays in H<sub>2</sub>O production due to slow H<sub>2</sub>O desorption or H<sub>2</sub>O adsorption in the transfer line may well also account for the observed phenomena.

**3.3. H<sub>2</sub> Chemisorption.** The H<sub>2</sub> adsorption measurements were carried out at -80 and 25 °C, in the low H<sub>2</sub> pressure region (2–20 Torr). The choice of this range of pressures was motivated both by the fact that hydrogen adsorption on the support is minimized under these conditions and by the possibility of the extension of the present methodology to other platinum group metals, for example, Pd. At certain temperatures

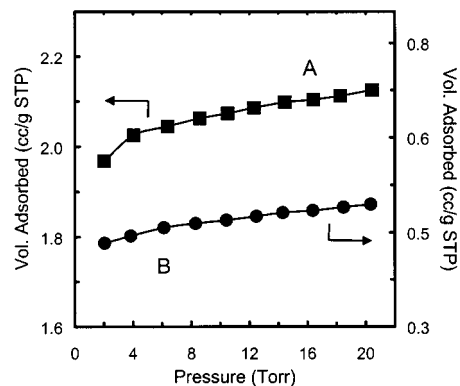


**Figure 4.** H<sub>2</sub> adsorption isotherms obtained at 25 °C (A) and -80 °C (B) on Rh/Ce<sub>0.68</sub>Zr<sub>0.32</sub>O<sub>2</sub> reduced at 150 °C.

and at high H<sub>2</sub> pressure, Pd may absorb hydrogen into the bulk, making reliable Pd dispersion measurements by H<sub>2</sub> adsorption impossible.<sup>1</sup>

We have also studied the hydrogen chemisorption on the Rh/CZ catalyst under pulse conditions. This technique is often used to measure the NM dispersion. A H/Rh value of 3.95 was obtained at room temperature. Attempts to discriminate the contribution of spilt-over hydrogen from that adsorbed on Rh showed a critical influence of several factors such as: (a) adsorption temperature, (b) volume and concentration of the H<sub>2</sub> pulse, and (c) delay between H<sub>2</sub> pulses. These factors did not allow definition of standard conditions for reliable detection of “true” H/Rh data.

In Table 1, values for Rh dispersion obtained from the volumetric study of hydrogen adsorption on the Rh/CZ catalyst are compared with values estimated from the HRTEM data. It can be seen from the table that there is excellent agreement between the results for H<sub>2</sub> chemisorption at -80 °C and the HRTEM data when  $T_{\text{red}} = 150, 350$  and 500 °C. This strongly supports the suggestion that reliable measurements of the H:Rh ratio are obtained when this low-temperature methodology is used. When the chemisorption experiments are performed at 25 °C, however, the H:Rh ratios obtained for  $T_{\text{red}} = 350$  °C and particularly  $T_{\text{red}} = 150$  °C are higher than those obtained for chemisorption at -80 °C. Typical H<sub>2</sub> adsorption isotherms obtained at -80 and 25 °C for Rh/CZ reduced at 150 °C are reported in Figure 4. Significantly higher amounts of H<sub>2</sub> are adsorbed at 25 °C compared to -80 °C, indicating the occurrence of extensive spillover of hydrogen species onto the support. For  $T_{\text{red}} = 500$  °C, the dispersion values obtained from the HRTEM data and the chemisorption experiments at both -80 and 25 °C are in almost perfect agreement. However, for  $T_{\text{red}} > 500$  °C, the values given by the two chemisorption methodologies remain in good agreement with each other but fall below the values obtained by the HRTEM technique. This suggests that H<sub>2</sub> adsorption at metal sites is partially blocked or deactivated by some process occurring at these high reduction temperatures.

Further insight can be gained by considering the equilibration times of H<sub>2</sub> adsorption under these different conditions. To enhance the sensitivity to the spillover phenomena, we have chosen rather rigorous criteria for the definition of the equilibrium conditions. In principle, discrimination of H<sub>2</sub> adsorption on the NM and on the support, via spillover of hydrogen species, can be made mainly on the basis of the rate of the two processes<sup>9</sup> because the latter process is in fact an activated one and therefore slower. We observed that for reduction temperatures below 500 °C, the attainment of the equilibrium conditions at 25 °C is

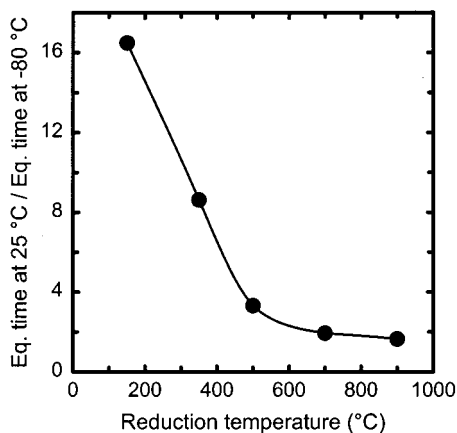


**Figure 5.** Ratio of time to reach equilibrium at H<sub>2</sub> pressure of 2 Torr at 25 °C to that measured at -80 °C versus temperature of reduction. Equilibrium conditions: see *Experimental Section*.

extremely slow, particularly at low hydrogen pressures. In contrast, for all the measurements carried out at -80 °C and those measured after a reduction at  $T_{\text{red}} \geq 500$  °C, the equilibrium conditions were attained quickly, after approximately 20 min. The ratio of equilibration time at 25 °C to that measured at -80 °C is plotted in Figure 5 versus reduction temperature. The H/Rh ratios measured at 25 °C substantially exceed those measured at -80 °C for reduction temperatures of 150 and 350 °C. These results agree with those of Table 1 in strongly suggesting that substantial spillover occurs at 25 °C for  $T_{\text{red}} = 150$  °C and  $T_{\text{red}} = 350$  °C, but that the extent of spillover decreases sharply with increasing  $T_{\text{red}}$ . Almost equal equilibration times are observed for reduction temperatures  $T_{\text{red}} \geq 500$  °C for both adsorption temperatures, suggesting comparable rates of H<sub>2</sub> adsorption. This could be taken as an indication that hydrogen adsorption is occurring almost exclusively on the metal center under the present experimental conditions. Nonactivated chemisorption should be expected for this process.

Reduction at 500 °C partially dehydroxylated the CeO<sub>2</sub> surface in a Rh/CeO<sub>2</sub> catalyst,<sup>27</sup> decreasing the rate of hydrogen transfer to the support. As a consequence, a good agreement of the H/Rh measured at -80 and at 25 °C was observed.<sup>27</sup> This phenomenon would explain the fall in spillover at 25 °C as  $T_{\text{red}}$  increases in the present work.

Notice that the choice of the experimental conditions, and particularly that of H<sub>2</sub> pressures and equilibrium criteria, is critical. Here conditions were chosen so as to minimize spillover phenomena. In a parallel investigation of H<sub>2</sub> activation over Rh/CeO<sub>2</sub>-ZrO<sub>2</sub> systems, where higher H<sub>2</sub> pressures were used, we observed that at a pressure of 30 Torr of H<sub>2</sub>, the equilibration time is twice as long at 25 °C as at -80 °C when Rh(NO<sub>3</sub>)<sub>3</sub> is used as precursor. In contrast, over a RhCl<sub>3</sub> precursor these differences were negligible.<sup>15</sup>

The fact that H/Rh values obtained by chemisorption for high reduction temperatures are lower than the corresponding values obtained by HRTEM may be explained by several phenomena. Hydrogen adsorption capability of the catalyst may decrease at these temperatures because of a strong metal support interaction-type phenomenon (either decoration of the metal particles by the support or an electronic effect), metal particle encapsulation, or metal particle sintering.<sup>25,28</sup> Particle sintering does occur and was detected in the particle size analyses of the HRTEM images. Although this sintering caused the fall in HRTEM dispersion values with increasing  $T_{\text{red}}$  seen in Table 1, it would have a similar effect on the H/Rh values obtained from the chemisorp-

tion experiments. It cannot, therefore, explain the difference between the two.

Encapsulation of Rh into the Ce<sub>0.68</sub>Zr<sub>0.32</sub>O<sub>2</sub> particles between fusing crystals or due to pore collapse because of support sintering during the reduction treatments can be reasonably ruled out by the fact that an extremely limited variation of surface areas were detected in these experiments by in situ BET measurements. Surface areas of 23.3, 20.8, and 20.1 m<sup>2</sup> g<sup>-1</sup> were measured for samples reduced at 150, 700, and 900 °C, respectively. Further, no appreciable change of the porosity of the sample after reduction at 700 °C was detected, as expected given the textural stability and limited porosity of the support.<sup>29</sup>

To ascertain which phenomenon is likely to occur under our experimental conditions, the effect on the samples of a moderate temperature reoxidation (427 °C) and a low temperature (150 °C) rereduction was investigated (Table 1, runs 5 and 7). When such a sequence of treatments was performed after reduction at both 700 and 900 °C, a remarkable agreement with the HRTEM data of the "reduced only" sample was again obtained. The value of H/Rh<sub>T</sub> = 0.23 after reduction at 900 °C is about 30% lower than that observed by HRTEM. Because particle decoration was observed for less than 5% of all the Rh particles imaged, we suggest that electronic effects may also play a role in this decrease of H/Rh. Some recent studies of nanostructural properties of NM/CeO<sub>2</sub> (NM = Rh<sup>30</sup> and Pt<sup>21</sup>) showed that the recovery of the metal particles from a decorated state or their redispersion requires reoxidation temperatures well above 500 °C. This suggests an electronic contribution to the metal-support interaction effects as detected in NM/CeO<sub>2</sub> reduced with H<sub>2</sub> at moderate temperatures.<sup>21</sup> A detailed study of these effects is needed to fully ascertain their origin in the Rh/CZ systems.

#### 4. Concluding Remarks

In summary, the present data show that measurement of true H/Rh ratios and hence estimation of Rh particle size in a Rh/Ce<sub>0.68</sub>Zr<sub>0.32</sub>O<sub>2</sub> sample can be achieved by means of volumetric H<sub>2</sub> chemisorption measurements, provided that an appropriate methodology is used that discriminates between the contributions of the support and of the metal. A criterion to ascertain the presence of a significant contribution from spillover hydrogen species to the adsorbed volumes is suggested. A reliable estimation of H/Rh can be obtained using (a) low H<sub>2</sub> pressures ( $P \leq 20$  Torr) and adsorption temperature ( $T = -80$  °C), (b) restrictive criteria for the definition of the equilibrium conditions, and (c) reduction pretreatment of the sample at moderate temperatures ( $T \leq 500$  °C).

At higher reduction temperatures, deactivation effects upon H<sub>2</sub> adsorption should be considered. However, a relatively mild reoxidation at 427 °C followed by a reduction at 150 °C reactivates the Rh chemisorption capability, which again allows *reliable* H/Rh ratios to be obtained. The fact that only very limited decoration of the Rh particles is observed by HRTEM after reduction at high temperatures suggests that electronic metal-support interactions, as discussed above, may play an important role in the chemical deactivation observed here. Work is in progress to ascertain the validity of this methodology for use with other NM.

**Acknowledgment.** The present paper has received financial support from the TMR Program of the European Commission (contract FMRX-CT-96-0060). Financial support from University of Trieste, the Ministero dell'Ambiente (Roma), contract no. DG 164/SCOC/97, Regione Friuli Venezia-Giulia "Fondo regionale per la ricerca", the CICYT (contract no.: MAT99-0570), and the Junta de Andalucia are also acknowledged.

## References and Notes

- (1) Anderson, J. R. *Structure of Metallic Catalysts*; Academic Press: London, 1975.
- (2) Heck, R. M.; Farrauto, R. J. *Catalytic Air Pollution Control. Commercial Technology*; Van Nostrand Reinhold: New York, 1995.
- (3) Kaspar, J.; Fornasiero, P.; Graziani, M. *Catal. Today* **1999**, *50*, 285.
- (4) Taylor, K. C. *Automobile Catalytic Converters. Catalysis—Science and Technology*; Anderson, J. R., Boudart, M., Eds.; Springer-Verlag: Berlin, 1984; Chapter 5.
- (5) Taylor, K. C. *Catal. Rev.—Sci. Eng.* **1993**, *35*, 457.
- (6) Shelef, M.; Graham, G. W. *Catal. Rev.—Sci. Eng.* **1994**, *36*, 433.
- (7) Nunan, J. G.; Robota, H. J.; Cohn, M. J.; Bradley, S. A. *J. Catal.* **1992**, *133*, 309.
- (8) Bernal, S.; Calvino, J. J.; Cifredo, G. A.; Rodriguez-Izquierdo, J. M.; Perrichon, V.; Laachir, A. *J. Chem. Soc. Chem. Commun.* **1992**, 460.
- (9) Bernal, S.; Calvino, J. J.; Cifredo, G. A.; Rodriguez-Izquierdo, J. M.; Perrichon, V.; Laachir, A. *J. Catal.* **1992**, *137*, 1.
- (10) Bernal, S.; Botana, F. J.; Calvino, J. J.; Cauqui, M. A.; Cifredo, G. A.; Jobacho, A.; Pintado, J. M.; Rodriguez-Izquierdo, J. M. *J. Phys. Chem.* **1993**, *97*, 4118.
- (11) Trovarelli, A.; Dolcetti, G.; de Leitenburg, C.; Kaspar, J.; Finetti, P.; Santoni, A. *J. Chem. Soc., Faraday Trans.* **1992**, *88*, 1311.
- (12) Fornasiero, P.; Kaspar, J.; Graziani, M. *J. Catal.* **1997**, *167*, 576.
- (13) Fornasiero, P.; Kaspar, J.; Sergio, V.; Graziani, M. *J. Catal.* **1999**, *182*, 56.
- (14) Bernal, S.; Calvino, J. J.; Cifredo, G. A.; Gatica, J. M.; Perez-Omil, J. A.; Laachir, A.; Perrichon, V. *Stud. Surf. Sci. Catal.* **1995**, *96*, 419.
- (15) Fornasiero, P.; Hickey, N.; Kaspar, J.; Dossi, C.; Gava, D.; Graziani, M. *J. Catal.* **2000**, *189*, 326.
- (16) Trovarelli, A. *Catal. Rev.—Sci. Eng.* **1996**, *38*, 439.
- (17) Bensalem, A.; Muller, J. C.; Tessier, D.; Bozon-Verduraz, F. *J. Chem. Soc., Faraday Trans.* **1996**, *92*, 3233.
- (18) Holmgren, A.; Andersson, B.; Duprez, D. *Appl. Catal., B* **1999**, *22*, 215.
- (19) Fajardie, F.; Tempere, J. F.; Djega-Mariadassou, G.; Blanchard, G. *J. Catal.* **1996**, *163*, 77.
- (20) Bernal, S.; Calvino, J. J.; Cauqui, M. A.; Perez-Omil, J. A.; Pintado, J. M.; Rodriguez-Izquierdo, J. M. *Appl. Catal., B* **1998**, *16*, 127.
- (21) Bernal, S.; Calvino, J. J.; Cauqui, M. A.; Gatica, J. M.; Larese, C.; Omil, J. A. P.; Pintado, J. M. *Catal. Today* **1999**, *50*, 175.
- (22) Colon, G.; Pijolat, M.; Valdivieso, F.; Vidal, H.; Kaspar, J.; Finocchio, E.; Daturi, M.; Binet, C.; Lavalley, J. C.; Baker, R. T.; Bernal, S. *J. Chem. Soc. Faraday Trans.* **1998**, *94*, 3717.
- (23) Daturi, M.; Binet, C.; Lavalley, J. C.; Vidal, H.; Kaspar, J.; Graziani, M.; Blanchard, G. *J. Chem. Phys.* **1998**, *95*, 2048.
- (24) Colon, G.; Valdivieso, F.; Pijolat, M.; Baker, R. T.; Calvino, J. J.; Bernal, S. *Catal. Today* **1999**, *50*, 271.
- (25) Bernal, S.; Botana, F. J.; Calvino, J. J.; Cifredo, G. A.; Perez-Omil, J. A. *Catal. Today* **1995**, *23*, 219.
- (26) Bernal, S.; Blanco, G.; Calvino, J. J.; Cifredo, G. A.; Perez-Omil, J. A.; Pintado, J. M.; Varo, A. *Stud. Surf. Sci. Catal.* **1994**, *82*, 507.
- (27) Bernal, S.; Calvino, J. J.; Cifredo, G. A.; Laachir, A.; Perrichon, V.; Herrmann, J. M. *Langmuir* **1994**, *10*, 717.
- (28) Badri, A.; Binet, C.; Lavalley, J. C. *J. Chem. Soc., Faraday Trans.* **1996**, *92*, 1603.
- (29) Pijolat, M. Personal communication, 1999.
- (30) Pfau, A.; Sanz, J.; Schierbaum, K. D.; Gopel, W.; Belzunegui, J. P.; Rojo, J. M. *Stud. Surf. Sci. Catal.* **1996**, *101*, 931.